Optimized Plasmonic Refractive Index Sensor Based on Graphene Ribbon Array

Alireza Dolatabady[a,*] and Nader Habibi[b]

[a]Department of Electrical Engineering, Faculty of Engineering, Ayatollah Boroujerdi University, Boroujerd, Iran
[b]Department of Mathematics, Faculty of Science, Ayatollah Boroujerdi University, Boroujerd, Iran

Corresponding author email: alireza.dolatabady@abru.ac.ir

ABSTRACT—In this paper, a plasmonic refractive index sensor based on a graphene ribbon array is proposed. Graphene ribbons are employed to excite surface plasmon waves, providing a subwavelength sensor. The structure exhibits a resonance feature, enabling wavelength-selective operation. It acts like a band rejection filter. The filtering behavior depends on the absorption of the incident light from an incident port at specific wavelengths. The rejected and absorbed bands depend on the structural parameters of the proposed sensor, such as the refractive index of the material surrounding the ribbons. A change in the refractive index of the material would change the wavelength of the transmitted lightwaves out of the sensor, providing a measuring approach to detect various transparent materials. The operation of the structure is simulated using the finite difference time domain (FDTD) numerical method and verified utilizing a simple characteristic equation. Due to the chemical potential dependency of graphene conductivity, the proposed sensor can be calibrated via an external voltage bias. The optimization of the proposed sensor performance can be accomplished through straightforward utilization of calculus. The proposed subwavelength sensor is widely applicable in terahertz-band applications, such as biological and chemical sensing.

KEYWORDS: Graphene ribbon, Optimization of sensor, Plasmonic structure, Refractive index sensor, Subwavelength structure, Wavelength selective structure.

I. INTRODUCTION

Metamaterials, artificially designed structures providing exciting features such as negative refractivity [1] and invisibility [2], have been employed in various configurations capable of tailoring the electromagnetic waves' characteristics not achievable with natural materials, such as in applications of cloaking [3, 4], antenna designing [5], and high-resolution optical imaging [6]. During recent years, the prosperous development of two-dimensional materials has led to many metasurface formations possessing outstanding features analogous to the former bulky metamaterials [7]. As the prior generation of two-dimensional materials, graphene, a single layer and a hexagonally sp[2]-bounded arrangement of carbon atoms [8], has motivated researchers towards graphene based metasurface structures investigation [9, 10] due to its remarkable mechanical [11], thermal [12], electrical [13], and optical [14] characteristics. So far, various graphene-based components of waveguides [15], couplers [16], circulators [17] and logic gates [18] have been proposed and investigated. Also, a variety of structures based on graphene metasurfaces by creating various kinds of patterns on the graphene layers has been analyzed and implemented [19]-[22]. Among these devices, filters are considered as one of the most crucial components in photonic systems. Thus far, myriad graphene-based filters and other wavelength selective structures based on different kinds of patterned

metasurfaces have been proposed, analyzed numerically, and investigated experimentally [23], [24]. Utilizing the variable response of the wavelength selective structures, via a change in various physical and structural parameters, can realize various sensors [25], [26]. For example, upon the variation of temperature in an elaborately designed structure, the central wavelength of a wavelength selective structure changes, which can provide a useful temperature sensor [25]. The other feasible sensor, which can be implemented through employing the variable response of wavelength selective structures, is a refractive index sensor. Recognizing different materials and finding out the density of solutions are inevitable in diverse applications, which can be covered by measuring the refractive index of the materials. So far, various refractive index sensors based on wavelength selective structures, including resonators, have been proposed and investigated [27], [28].

In this paper, a refractive index sensor based on the structure of a band-stop filter including a periodic arrangement of graphene nano-ribbons is proposed. The structure behaves as a simple wavelength selective metasurface whose central wavelength depends on the resonance wavelength of the ribbon array, which in turn is dependent on the effective permittivity of the medium surrounding the graphene ribbon array [29]. In this structure, graphene plays the main role of waveguiding and supports tunable and extremely confined plasmons, which makes it possible to provide a sub-wavelength component and overcomes the diffraction limit of light. The performance of the proposed structure is investigated through simulations using the finite difference time domain (FDTD) numerical method. Due to the tunability of graphene conductivity via changes in its chemical potential, the sensor can be calibrated for the desired applications. The sensitivity and modulation depth, as two operational criteria, are defined, and some practical considerations are investigated. Also, a comparison between the proposed sensor and some recently investigated refractive index sensors is carried out. In addition, basic calculus derivative is employed to optimize the performance of the

sensor in terms of some physical and structural parameters. Finally, an application as a sensor for the identification of various alcohols is proposed.

The remaining of the paper is organized as follows: In Section II, the basic structure is proposed and its analytic description is presented. In Section III, the simulation results of the sensor investigation are presented and discussed. In Section IV, some practical considerations are discussed. Section V studies the optimization of the proposed structure based on basic calculus derivatives. Section VI represents a special application of the proposed sensor as a discriminator of various alcohols. Finally, the paper is concluded in Section VII.

II. THE PROPOSED STRUCTURE AND ITS ANALYTIC DESCRIPTION

The three-dimensional schematic view of the proposed structure is exhibited in Fig. 1. The unit cell structure is composed of a rectangular graphene nanoribbon deposited over a silicon-on-insulator substrate. The thickness and relative electric permittivity of the silicon part of the substrate are denoted as h and ε_s, respectively. The whole structure is a periodic arrangement of the unit cell along the longer axis of the ribbon (z axis, according to Fig. 1). The width of ribbons and the lattice constant are represented by w and a, respectively. The length of each ribbon is assumed to be infinite (in practice, more than ten times longer than the ribbon's width). According to Fig. 1, there are two ports, as incident and transmission, in the upper and lower parts of the structure, respectively. The periodic array of graphene ribbons is excited by a plane wave normally incident on the structure from the upper port. The transmitted power is detected in the lower port. After the incident of lightwaves toward graphene ribbons, they would be absorbed except in specific resonance wavelengths of the structure, which would transmit toward the lower port. So, some specific wavelengths can be detected in the transmission port. The resonance wavelengths of the structure depend on the electric permittivity of the material surrounding the graphene ribbons, and so, their

refractive index. Therefore, a change in the surrounding material can lead to a change in resonance wavelengths, the idea used to design the proposed refractive index sensor.
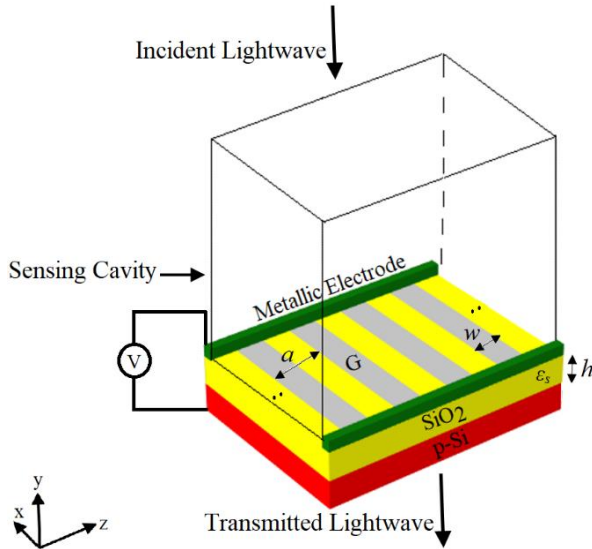

Fig. 1. Schematic view of the proposed sensor structure. w, a, and h denote the width of graphene layers, the lattice constant of the periodic arrangement of graphene layers, and the thickness of the SiO$_2$ part of the substrate, respectively. G specifies the graphene layers. The gate voltage is applied between the substrate and graphene layers, through two metallic electrodes. The material under recognition is injected into the sensing cavity. "..″s in two sides over the substrate imply a periodic arrangement of graphene layers. An incident lightwave from a specific source propagates towards the structure and finally transmits toward a detection device.

To investigate the operation of the proposed sensor, the Kubo formula has been utilized to express graphene conductivity as a dispersive material containing inter- and intra-band transitions as [18]:

$$\sigma_g = \frac{-je^2 k_B T}{\pi \hbar^2 \left(\omega - j\tau^{-1}\right)} \left\{ \frac{\mu_c}{k_B T} + 2\ln\left[\exp\left(-\frac{\mu_c}{k_B T}\right) + 1 \right] \right\}$$
$$-j\frac{e^2}{4\pi\hbar^2} \ln\left[\frac{2|\mu_c| - \hbar\left(\omega - j\tau^{-1}\right)}{2|\mu_c| + \hbar\left(\omega - j\tau^{-1}\right)} \right] \quad (1)$$

where j, e, T, k_B, τ, μ_c, $\hbar$, and ω, respectively signify imaginary unit, electron charge, temperature, Boltzmann's constant, carrier relaxation time, chemical potential, reduced Planck's constant, and angular frequency. For

highly doped graphene, at room temperature, and for terahertz frequencies, the inter-band term is negligible and Eq. (1) is shortened as the following Drude-like term [18]:

$$\sigma_g = \frac{-je^2 \mu_c}{\pi \hbar^2 \left(\omega - j\tau^{-1}\right)}, \quad (2)$$

The resonance wavelength of the structure, including the single-layer graphene ribbon array as a function of the graphene ribbon width and chemical potential, can be deduced from a quasi-static analysis as the following simple characteristic equation [29]:

$$\lambda_r \approx \frac{2\pi c\hbar}{e} \sqrt{\frac{\eta \varepsilon_{eff} \varepsilon_0 w}{\mu_c}}, \quad (3)$$

where c, ε_0, and w, denote the free space speed of light, vacuum electric permittivity, and the width of ribbons, respectively. ε_{eff} is the effective permittivity of the media surrounding the graphene ribbon array as the average value of the permittivities over and under the graphene ribbons, i.e., $\varepsilon_{eff} = (\varepsilon_{MUR} + \varepsilon_s)/2$, where ε_{MUR} and ε_s are the electric permittivities of the material under recognition and substrate, respectively. The dimensionless constant $\eta=3.1$ is a fitting parameter derived from numerical simulations. Equation (3) implies that the resonance wavelength of the structure depends on the refractive index of the material over graphene ribbons, n, since $n^2=\varepsilon_{MUR}$.

III. THE SIMULATION RESULTS

To carry out the simulations, graphene is defined with the following in-plane equivalent dielectric permittivity [18]:

$$\varepsilon_{eq} = \varepsilon_{gr} - j\frac{\sigma_g}{\omega\varepsilon_0 \Delta}, \quad (4)$$

where ε_{gr} and Δ denote the relative permittivity perpendicular to the graphene sheet and graphene thickness, respectively. All of the structural and physical parameters are given in the Table. 1. To implement simulation results, Maxwell equations are solved based on the FDTD method, using Lumerical commercial

package, with periodic boundary conditions in the x-z directions. To guarantee the convergence, the grid sizes in *x*, *y*, and z directions are taken to be 10, 10, and 0.5 nm, respectively. The incident wave is incident perpendicular to the structure.
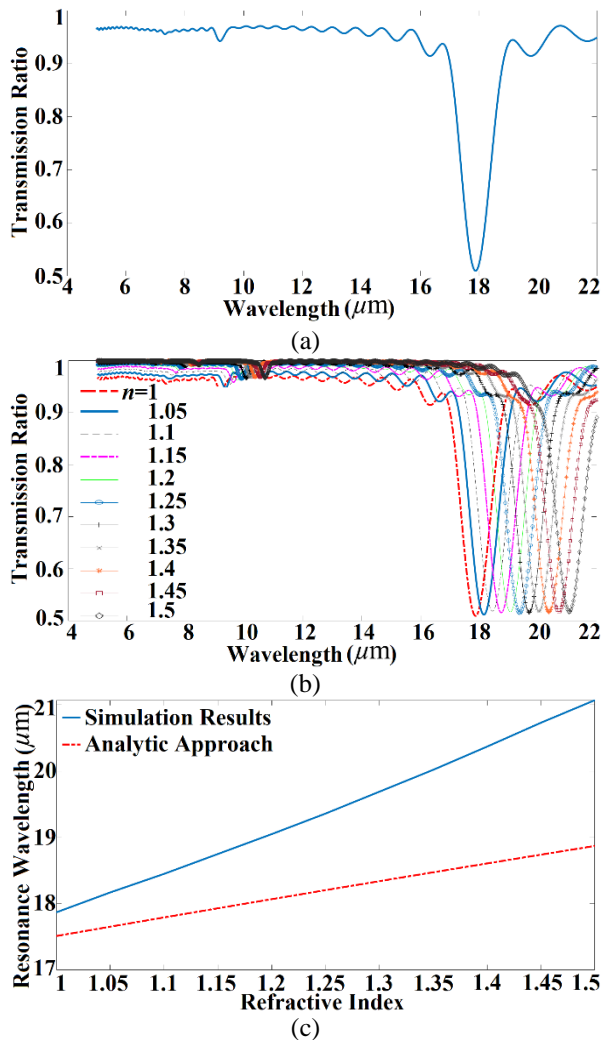

(a)

(b)

(c)

Fig. 2. (a) Simulation results for power transmission ratio spectrum of the proposed structure in Fig. 1 while the refractive index of material inside the cavity is assumed to be 1. (b) Simulation results for power transmission ratio spectra of the proposed structure for various amounts of refractive index of the materials inside the cavity. (c) The resonance wavelength versus refractive index of the materials inside the cavity based on simulation and analytic approaches. There is a linear relation between refractive index and resonance wavelength.

Figure 2(a) shows the simulation results for the power transmission ratio. As it is clear, there is a dip in transmission in the vicinity of the central frequency (λ_r) of 17.87 μm, providing a band rejection feature of the structure. The value of full width at half maximum (FWHM),

is equal to 1.15 μm. These two parameters of resonance frequency (λ_r) and bandwidth, or equivalently, FWHM, are often used to characterize the performance of wavelength-selective structures. The quality factor, defined as the ratio of the resonance wavelength to the full width at half maximum (Q= λ_r/FWHM), is 15.54. Table 1 demonstrates that the nanoribbon width is significantly smaller than the operating wavelength.

Therefore, the proposed structure behaves as a subwavelength waveguiding component in the terahertz regime. Figure 2(b) shows the spectra of transmission ratio for various refractive indices of material over the graphene ribbons. Figure 2(c) illustrates the relationship between the refractive index and the resonance wavelength, derived from the simulation results of Figure 2(b) and the analytical model of (3).

Figure 2(c) demonstrates that the refractive index change in the surrounding material alters the resonance wavelength in a quasi-linear manner. Therefore, the measurement of the resonance wavelength of the structure can be a good method to sense the change in the material around the structure and to recognize a material based on a previously designed lookup table. This material is assumed to be injected into the sensing cavity according to Fig. 1.

Table 1. The structural and physical parameters for simulation investigation of the proposed structure of Fig. 1.

w	a	μ_c	τ	h	Δ	ε_s	ε_{gr}	V_F
150 nm	300 nm	0.2 eV	0.6 ps	50 nm	1 nm	2.1	2.5	10^6 m/s

IV. SOME PRACTICAL CONSIDERATIONS

As the Kubo formula implies, graphene conductivity depends on the chemical potential. Therefore, to change in chemical potential can lead to a change in resonance wavelength. Figure 3(a) exhibits simulated transmission spectra of the structure for various amounts of graphene chemical potentials. An increase in chemical potential leads to a blue shift of the transmission spectra. Hence, the chemical

potential of the graphene layers, as one of the influential factors on the graphene layer conductivity, can tune the resonance wavelength of the proposed structure and also can calibrate the sensor for the demanded applications. One procedure to change the chemical potential is to use an external voltage applied to the graphene layer, via the following relation [30]:

$$\mu_c = \hbar V_F \sqrt{\frac{\pi \varepsilon_0 \varepsilon_s V_B}{eh}} \, , \qquad (5)$$

where V_F denotes the Fermi velocity. According to Fig. 1 and based on (5), applying an external voltage gate can tune the chemical potential, as illustrated in Fig. 3(b). Figure 3(c) illustrates the resonance wavelength shift as a function of the chemical potential, derived from simulated and analytical models. Consequently, the sensor's resonance wavelength must be tuned to fall within the optimal spectral range of the detection system, due to the system's spectral constraints. It can be realized by varying the chemical potential of the graphene to change its conductivity.

To investigate the overall performance of the proposed sensor, two parameters of sensor sensitivity (*SS*), the rate of variation of the structure resonance wavelength with respect to refractive index of the material inside the sensing cavity, in micrometers per refractive index unit, and sensing resolution (*SR*) are defined as follows:

$$SS = \frac{d\lambda_r}{dn}, \quad SR = \left(\frac{dn}{d\lambda_r}\right)\Delta\lambda \, , \qquad (6)$$

where $\Delta\lambda$ is the wavelength resolution of the detection system, employed at the transmission port. According to the simulation results of Fig. 2(c), for the sensor designed by the parameters given in Table 1, *SS* can be calculated as 5.4 micrometers per refractive index unit. For a detection system with a wavelength resolution of $\Delta\lambda = 1pm$, *SR* can be evaluated as 18×10^{-8} per refractive index unit. The other useful criterion is modulation depth (*MD*) defined as:

$$MD = \left| \frac{T_{max} - T_{min}}{T_{max}} \right| , \qquad (7)$$

where T_{max} and T_{min} denote maximum and minimum values of power transmission according to Fig. 2(a), respectively. According to the simulation results of Fig. 2(a), *MD* can be calculated as 0.48 (-3.2 dB).

As observed in Fig. 3(c), a higher chemical potential (and thus a larger carrier concentration) results in a significantly higher MD, which enables the use of less sensitive detection systems.

To utilize the sensor, injection of the target material (analyte) into the structural cavity is required (as depicted in Fig. 1(a)), thereby modifying the dielectric medium surrounding the graphene ribbons. To achieve precise results, the sensor should be appropriately calibrated. The material recognition process is conducted in two steps: First, a lookup table is established for the designed sensor, containing reference pairs of known refractive indices and their corresponding resonance wavelengths. Subsequently, the sensed material (analyte) is identified by matching its measured wavelength to this table. Also, it should be remembered that the sensing cavity should be uncontaminated before every usage. In addition, the material should not etch the structure and interact with graphene and silica.

Based on the refractive index detection feature of the proposed structure, it can be promoted as a sensor for various other applications, such as the identification of blood groups, oil components, and proteins. It can also be promoted to a temperature sensor via proper design. As a simple clarification of the temperature dependency of the refractive index, it should be mentioned that temperature can change the density of the material, and therefore, change its refractive index [28].

The proposed structure can be practically implemented based on various procedures [31]-[33]. For example, microcleaving of highly oriented pyrolytic graphite (HOPG) can

provide single and few-layer graphene flakes, which are next transferred into SiO₂/Si substrates. Also, due to recent developments of THz sources, it can be possible to excite the structure to propagate lightwaves according to the spectra shown in Fig. 2(a) [34].
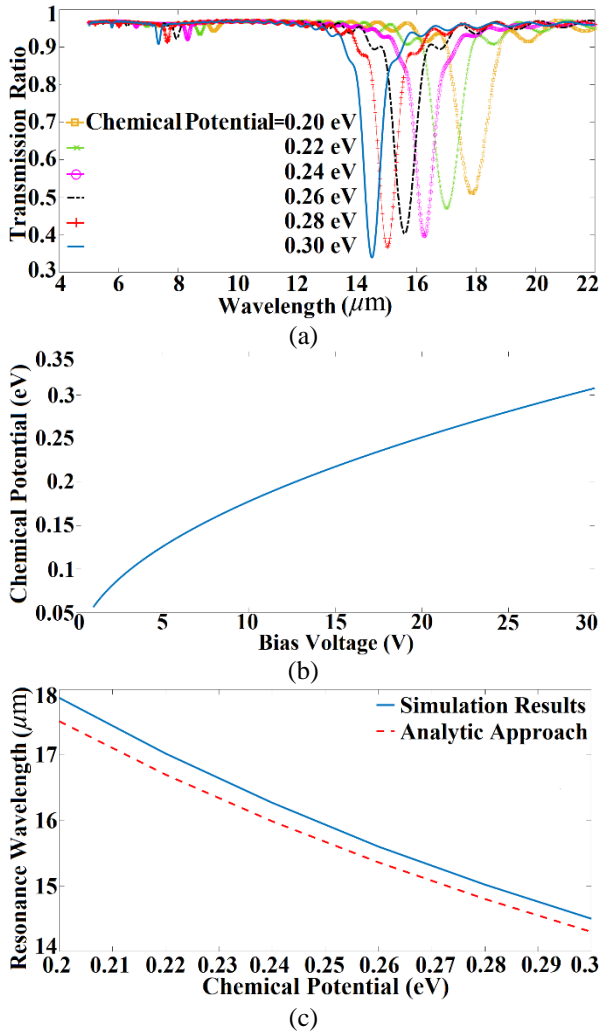

(a)

(b)

(c)

Fig. 3. (a) Simulated transmission spectra of the structure for various amounts of graphene chemical potentials. (b) The relation between the graphene layer chemical potential and the applied external gate voltage. (c) The relation between resonance wavelength and chemical potential of graphene ribbons based on simulation and analytic approaches.

V. OPTIMIZATION OF THE PROPOSED STRUCTURE

To yield the maximum wavelength shift with respect to the change in refractive index, the adjustment of two parameters of chemical potential and ribbon width, can be used. Therefore, an optimization problem should be addressed to maximize the multivariable

function of $\partial\lambda_r/\partial n$ [35]. During the optimization, as a fundamental mathematical approach for determining the best possible solution to a given problem, and based on (3), the following objective function is maximized [36]:

$$\frac{\partial\lambda_r}{\partial n}\left(n,\mu_c,w\right)=\frac{2\pi c\hbar n}{e\sqrt{n^2+\varepsilon_s}}\sqrt{\frac{\eta\varepsilon_0 w}{2\mu_c}},\qquad(8)$$

subject to the constraints of $0.01\leq\mu_c\leq1$ and $5\leq w\leq50$. Since $\lim_{n\to\infty}\dfrac{n}{\sqrt{n^2+\varepsilon_s}}=1$, the maximum

value is approximately attained when $\mu_c\leq0.01$ eV and $w=50$ nm. Therefore:

$$\frac{\partial\lambda_r}{\partial n}\left(n,0.01,50\right)\approx\frac{100\pi c\hbar}{e}\sqrt{\eta\varepsilon_0},\qquad(9)$$

Table 2. A comparison between the proposed sensor and some previously proposed sensors with a similar idea of sensing.

Ref.	Structure	The idea of sensing	Sensitivity (micrometers per refractive index unit)
28	two coupled graphene parallel plane waveguides	surface plasmon resonance	1.920
37	periodic gold nanotubes coupled with a gold film	surface plasmon resonance	1.002
38	nanoring-strip graphene arrays	surface plasmon resonance	5.20
39	gold rods over graphene layer	plasmonic perfect absorber	0.981
40	periodic Au rings array	surface plasmon resonance	0.557
41	Au covered silica sphere	surface plasmon resonance	0.968
42	Bragg grating based on photonic crystal fiber	surface plasmon resonance	0.487
43	Metallic nanoparticles with a Fabry-Perot cavity	surface plasmon resonance	0.600

According to the parameters of Table 1, (9) would lead to 81/02 micrometers per refractive index unit. However, this amount of sensor sensitivity is attained through using narrower graphene layers with lower chemical potential, which causes a more difficult process of fabrication and higher power loss. Table 2, expresses a comparison between the proposed sensor and some previously proposed ones with a similar idea of sensing in terms of sensor sensitivity.

VI. APPLICATION AS A DISCRIMINATOR OF VARIOUS ALCOHOLS

In various chemical industries, some kinds of alcohols are produced [44]. To recognize these products in an effective manner, meticulous analysis should be carried on. However, some of these analysis methods may be time-consuming and hazardous. Detecting and discriminating various alcohols can be achieved with the proposed refractive index sensor. So far, various refractive index sensors have been employed to detect diverse alcohols [45]. For instance, for different alcohols of methanol, ethanol, propanol, butanol, pentanol, hexanol, heptanol, and octanol, by increasing the number of carbon atoms in their compositions, the refractive index is incremental from 1.331 to 1.429 [46]. According to the results realized in Section 3, an increase in refractive index of the materials under investigation would lead to a redshift in resonance wavelength. It can identify a specific alcohol via a suitably prepared lookup table.

VII. CONCLUSION

In this paper, a plasmonic refractive index sensor based on a graphene ribbon array is proposed. As a wavelength selective structure, the proposed component operation depends on the refractive index of the material surrounding the graphene ribbons. The well-known finite difference time domain numerical method is used to simulate the performance of the sensor. By applying a proper gate voltage for variation of the chemical potential of graphene ribbons can tune the provided response by the sensor to achieve the maximum sensitivity of the external detection device. The proposed subwavelength

sensor can be employed extensively in terahertz demanded applications such as bio- and chemical-systems and promoted to other useful sensors such as temperature sensors.

REFERENCES

[1] Y. Liu, G.P. Wang, J.B. Pendry, and S. Zhang, "All-angle reflectionless negative refraction with ideal photonic Weyl metamaterials," Light Sci. Appl. Vol. 11, pp. 276(1-7), 2022.

[2] X. Jing, D. Feng, Y. Tian, M. Li, C. Chu, C. Li, Y. He, H. Gan, and Z. Hong, "Design of two invisibility cloaks using transmissive and reflective metamaterial-based multilayer frame microstructures," Opt. Express, Vol. 28, pp. 35528-35539, 2020.

[3] M. Shaheryar Khan, R.A. Shakoor, O. Fayyaz, and E. Mahdi Ahmed, "A focused review on techniques for achieving cloaking effects with metamaterials," Optik, Vol. 297, pp. 171575(1-20), 2023.

[4] H. Nassar, Y.Y. Chen, and G.L. Huang, "Polar metamaterials: A new outlook on resonance for cloaking applications," Phys. Rev. Lett. Vol. 124, pp. 084301(1-6), 2020.

[5] C. Milias, R.B. Andersen, P.I. Lazaridis, Z.D. Zaharis, B. Muhammad, and J.T.B. Kris, "Metamaterial-inspired antennas: A review of the state of the art and future design challenges," IEEE Access, Vol. 9, pp. 89846-89865, 2021.

[6] R. Dhama, B. Yen, C. Palego, and Z. Wang, "Super-resolution imaging by dielectric super lenses: TiO_2 metamaterial super lens versus $BaTiO_3$superlens," Photonics, Vol. 8, pp. 222(1-9), 2021.

[7] M. Xu, T. Liang, M. Shi, and H. Chen, "Graphene-like two-dimensional materials," Chem. Rev. Vol. 113, pp. 3766-3798, 2013.

[8] A.R. Urade, I. Lahiri, and K.S. Suresh, "Graphene properties, synthesis and applications: A review," J. Min. Met. Met. Soc. Vol. 75, pp. 614-630, 2023.

[9] B. Wang, K. Gai, R. Wang, F. Yan, and L. Li, "Ultra-broadband perfect terahertz absorber with periodic-conductivity graphene metasurface," Opt. Laser Technol. Vol. 154, pp. 160-167, 2022.

[10] Z. Li, K. Yao, F. Xia, S. Shen, J. Tian, and Y. Liu, "Graphene plasmonic metasurfaces to steer infrared light," Sci. Rep. Vol. 5, pp. 12423(1-9), 2015.

[11] V.B. Mbayachi, E. Ndayiragije, T. Sammani, S. Taj, E.R. Mbuta, and A.U. Khan, "Graphene synthesis, characterization and its applications: A review," Results Chem. Vol. 3, pp. 100163(1-9), 2021.

[12] S. Chen, Q. Wu, C. Mishra, J. Kang, H. Zhang, K. Cho, W. Cai, A.A. Balandin, and R.S. Ruoff,

"Thermal conductivity of isotopically modified graphene," Nat. Mat. Vol. 11, pp. 203-207, 2012.

[13] K.S. Novoselov, V.I. Falko, L. Colombo, P.R. Gellert, M.G. Schwab, and K. Him, "A roadmap for graphene," Nature, Vol. 490, pp. 192-200, 2012.

[14] A.N. Grigorenko, M. Polini, and K.S. Novoselov, "Graphene plasmonics," Nat. Photon. Vol. 6, pp. 749-758, 2012.

[15] A. Dolatabady, N. Granpayeh, and M. Salehi, "Ferrite loaded graphene based plasmonic waveguide," Opt. Quant. Electron. Vol. 50, pp. 345(1-11), 2018.

[16] M. Gholipoor and N. Solhtalab, "Broadband graphene-based optical power coupler and polarization beam splitter using a directional coupler," OSA Continuum, Vol. 4, pp. 3221-3232, 2021.

[17] A. Dolatabady and N. Granpayeh, "Graphene based far-infrared junction circulator," IEEE Trans. Nanotechnol. Vol. 18, pp. 200-207, 2019.

[18] A. Dolatabady, N. Granpayeh, and M. Abedini, "Frequency-tunable logic gates in graphene nano-waveguides," Photon. Net. Commun., Vol. 39, pp. 187-194, 2020.

[19] A. Andryieuski and A.V. Lavrinenko, "Graphene metamaterials based tunable terahertz absorber: effective surface conductivity approach," Opt. Express, Vol. 21, pp. 9144-9155, 2013.

[20] R. Alaee, M. Farhat, C. Rockstuhl, and F. Lederer, "A perfect absorber made of a graphene micro-ribbon metamaterial," Opt. Express, Vol. 20, pp. 28017-28024, 2012.

[21] M. Faraji, M.K. Moravvej-Farshi, and L. Yousefi, "Tunable THz perfect absorber using graphene-based metamaterials," Opt. Commun. Vol. 355, pp. 352-355, 2015.

[22] A. Dolatabady and N. Granpayeh, "Manipulation of the Faraday rotation by graphene metasurfaces," J. Magn. Magn. Mater. Vol. 469, pp. 231-235, 2019.

[23] H.S. Chu and C.H. Gan, "Active plasmonic switching at mid-infrared wavelengths with graphene ribbon arrays," Appl. Phys. Lett. Vol. 102, pp. 68-72, 2013.

[24] H. Zhuang, F. Kong, K. Li, and S. Sheng, "Plasmonic bandpass filter based on graphene nanoribbon," Appl. Opt. Vol. 54, pp. 2558-2564, 2015.

[25] P. Ji, Q. Shi, L. Zheng, G. Wang, and F. Chen, "High sensitivity plasmonic refractive index and temperature sensor based on square ring shape resonator with nanorods defects," Opt. Quant. Electron. Vol. 54, pp. 184(1-15), 2022.

[26] Z. Chen, X. Ma, S. Zhang, T. Li, Y. Wang, and Z.L. Hou, "Pressure sensor based on optical resonator in a compact plasmonic system," IEEE Sens. J. Vol. 24, pp. 4418-4423, 2024.

[27] A. Dolatabady, N. Granpayeh, and V. Foroughi Nezhad, "A nanoscale refractive index sensor in two dimensional plasmonic waveguide with nanodisk resonator," Opt. Commun. Vol. 300, pp. 265-268, 2013.

[28] A. Dolatabady, S. Asgari, and N. Granpayeh, "Tunable mid-infrared nanoscale graphene-based refractive index sensor," IEEE Sens. J. Vol. 18, pp. 569-574, 2018.

[29] H.S. Chu and C.H. Gan, "Active plasmonic switching at mid-infrared wavelengths with graphene ribbon arrays," Appl. Phys. Lett. Vol. 102, pp. 231107(1-4), 2013.

[30] J.S. Gomez-Diaz and J. Perruisseau-Carrier, "Graphene-based plasmonic switches at near infrared frequencies," Opt. Express, Vol. 21, pp. 15490-15504, 2013.

[31] [31] B.K. Min, S.K. Kim, S.J. Kim, S.H. Kim, M.A. Kang, C.Y. Park, W. Song, A. Myung, J. Lim, and K.S. An, "Electrical double layer capacitance in a graphene embedded Al_2O_3 gate dielectric," Sci. Rep. Vol. 5, pp. 16001(1-7), 2015.

[32] M. Pan, Z. Liang, Y. Wang, and Y. Chen, "Tunable angle-independent refractive index sensor based on Fano resonance in integrated metal and graphene nanoribbons," Sci. Rep. Vol. 6, pp. 29984(1-9), 2016.

[33] [33] X. Yan, L. Yuan, Y. Wang, T. Sang, and G. Yang, "Transmittance characteristics and tunable sensor performances of plasmonic graphene ribbons," J. Phys. Chem. C, Vol. 112, pp. 17741-17744, 2008.

[34] R.A. Lewis, "A review of terahertz sources," J. Phys. D: Appl. Phys. Vol. 47, pp. 374001(1-11), 2014.

[35] D.G. Luenberger and Y. Yinyu, *Linear and Nonlinear Programming*, Springer Nature, 5th Ed. 2021.

[36] J. Hass, C. Heil, and M. Weir, *Thomas' Calculus: Early Transcendentals*, Pearson, 14th Ed. 2017.

[37] X. Wang, J. Zhu, X. Wen, X. Wu, Y. Wu, Y. Su, H. Tong, Y. Qi, and H. Yang, "Wide range refractive index sensor based on a coupled structure of Au nanocubes and Au film," Opt. Mat. Express, Vol. 9, pp. 3079-3088, 2019.

[38] C. Cen, H. Lin, J. Huang, C. Liang, X. Chen, Y. Tang, Z. Yi, X. Ye, J. Liu, Y. Yi, and S. Xiao, "A tunable plasmonic refractive index sensor with nanoring-strip graphene arrays," Sensors, Vol. 18, pp. 4489(1-10), 2018.

[39] M. Irfan, Y. Khan, A.U. Rehman, M.A. Butt, S.N. Khonina, and N.L. Kazanskiy, "Plasmonic refractive index and temperature sensor based on graphene and LiNbO₃," Sensors, Vol. 22, pp. 7790(1-12), 2022.

[40] S. Wang, X. Sun, M. Ding, G. Peng, Y. Qi, Y. Wang, and J. Ren, "The investigation of an LSPR refractive index sensor based on period gold nanoring array," J. Phys. D. Appl. Phys. Vol. 51, pp. 045101(1-7), 2018.

[41] B.B. Choi, B. Kim, Y. Chen, S.J. Yoo, Y. Cho, and P. Jiang, "Elevated surface plasmon resonance sensing sensitivity of Au-covered silica sphere monolayer prepared by Langmuir-Blodgett coating," J. Ind. Eng. Chem. Vol. 99, pp. 179-186, 2021.

[42] N. Wei, P. Xu, Y. Yao, J. Li, E. Liu, and J. Luo, "Bragg grating sensor for refractive index based on a D-shaped circular photonic crystal fiber," J. Opt. Soc. Am. Vol. 39, pp. 800-805, 2022.

[43] J. Chen, Q. Zhang, C. Peng, C. Tang, X. Shen, L. Deng, and G.S. Park, "Optical cavity-enhanced localized surface plasmon resonance for high-quality sensing," IEEE Phot. Technol. Lett. Vol. 30, pp. 728-731, 2018.

[44] V.R. Surisetty, A.K. Dalai, and J. Kozinski, "Alcohols as alternative fuels: An overview," Appl. Catal. A: Gen. Vol. 404, pp. 1-11, 2011.

[45] R. Rahad, N. Hossain, and A. Hossain, "Enhanced alcohol detection using surface plasmon polariton dependent MIM plasmonic sensor," Plasmonics, Vol. 20, pp. 1331-1340, 2025.

[46] J. Ortega, "Densities and refractive indices of pure alcohols as a function of temperature," J. Chem. Eng. Data, Vol. 27, pp. 312-317, 1982.

Alireza Dolatabady has received his B.Sc. degree in electrical and electronics engineering from Iran University of Science and Technology, Tehran, Iran, in 2010, and his M.Sc. and Ph.D. degrees in Telecommunication Engineering from K.N. Toosi University of Technology, Tehran, Iran, in 2012 and 2018, respectively. He is currently pursuing his research activities as an assistant professor in Ayatollah Boroujerdi University, Boroujerd, Iran. His research interests include photonic devices, plasmonic structures, and components based on two dimensional materials. Dr. Dolatabady is also a member of Institute of Electrical and Electronics Engineers (IEEE), Optical Society of Iran (OPSI) and Iranian Society of Engineering Education (ISEE).

Nader Habibi was born in Zanjan, Iran. He began his undergraduate studies in pure mathematics at Zanjan University, Zanjan, Iran in 1994 and pursued his master's degree in the same field in 2002. He defended his doctoral dissertation in 2014 and has been a faculty member of the Mathematics Department at Ayatollah Boroujerdi University, Boroujerd, Iran since October 2025. His research interests include graph theory, algebraic graph theory, and financial mathematics.

THIS PAGE IS INTENTIONALLY LEFT BLANK.